ARBITRARILY ORIENTED PERFECTLY MATCHED LAYER IN THE FREQUENCY DOMAIN

Xiaoming Xu and Robin Sloan
Department of Electrical Engineering and Electronics
UMIST, Manchester, M60 1QD, UK

ABSTRACT

An arbitrarily oriented PML is introduced by using complex space mapping, for more flexible meshing of microwave engineering problems. The PML can be oriented in any direction. The discussion is extended to two-direction PMLs for matching the interface between one-direction PMLs, and three-direction PMLs for two-direction ones. Numerical result is presented.

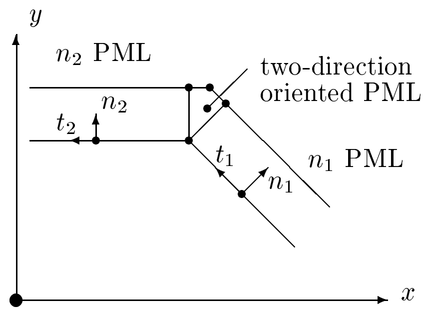

Figure 1: 2D Display of Arbitrarily Oriented PMLs

INTRODUCTION

Since Berenger [1] introduced a novel concept about a non-physical medium, Perfectly Matched Layer (PML), for absorbing propagating electromagnetic waves, a number of developments about its theory and application have been contributed by the community. Dozens of papers have been published on this topic, which are not cited here due to requirement for brevity. It has been noticed that most of the theoretical discussion and applications are limited to the orthodox PML structure in which PMLs are oriented along Cartesian coordinate axes. To remove this limitation from practical PML structures, especially for flexible finite element meshing, arbitrarily oriented PMLs are introduced by the authors. The facets of this kind of PML are still planes, but they can be oriented in any direction without limitation, as shown in Fig. 1. This characteristic provides more flexibility to construct PML structures fitting the complex geometry of engineering problems.

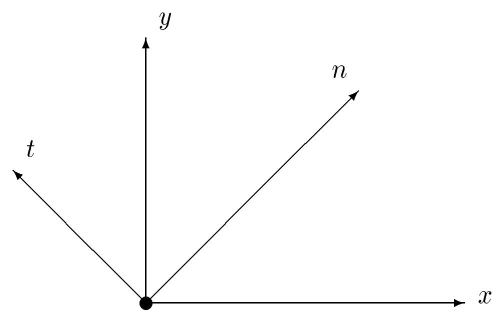

Figure 2: 2D Display of Rotated Coordinates

FORMULATION

To find the generalized differential operator for a one-direction PML oriented in the n direction, firstly the operator is defined in a new rectangular coordinate system (n, t, τ) as shown in Fig. 2, where $\hat{n} = \hat{x}n_x + \hat{y}n_y + \hat{z}n_z$, $\hat{t} = \hat{x}t_x + \hat{y}t_y + \hat{z}t_z$ and $\hat{\tau} = \hat{x}\tau_x + \hat{y}\tau_y + \hat{z}\tau_z$ are the unity vectors in normal and tangential directions respectively, by using complex mapping scale s_n along n direction, similar to mapping along the Cartesian coordinates [2, 3]. Then the definition is transformed into Cartesian coordinate system, which is the common coordinate system for various PMLs.

$$[\mathbf{D}]_1^n = \hat{n}\frac{1}{s_n}\frac{\partial}{\partial n} + \hat{t}\frac{\partial}{\partial t} + \hat{\tau}\frac{\partial}{\partial \tau} \quad (1)$$

$$= [\hat{x}, \hat{y}, \hat{z}] \; [\mathbf{D}]_1^n \begin{bmatrix} \frac{\partial}{\partial x} \\ \frac{\partial}{\partial y} \\ \frac{\partial}{\partial z} \end{bmatrix} \quad (2)$$

where the items of the matrix $[\mathbf{D}]_1^n$ are given in (8). Finally, a few identical relationships, $n_x^2 + t_x^2 + \tau_x^2 = 1$, $n_x n_y + t_x t_y + \tau_x \tau_y = 0$ and so on , are applied to obtain (9).

Similarly, the operator for two- and three- direction PMLs are derived as follows. The explanations of the matrices $[\mathbf{D}]_2^{n-t}$ and $[\mathbf{D}]_3^{n-t-\tau}$ are listed in (10) and (11). Details of the formulation will be provided in the full conference paper.

$$\nabla_2^{n-t} = \hat{n}\frac{1}{s_n}\frac{\partial}{\partial n} + \hat{t}\frac{1}{s_t}\frac{\partial}{\partial t} + \hat{\tau}\frac{\partial}{\partial \tau} \quad (3)$$

$$= [\hat{x}, \hat{y}, \hat{z}] \; [\mathbf{D}]_3^{n-t} \begin{bmatrix} \frac{\partial}{\partial x} \\ \frac{\partial}{\partial y} \\ \frac{\partial}{\partial z} \end{bmatrix} \quad (4)$$

$$\nabla_3^{n-t-\tau} = \hat{n}\frac{1}{s_n}\frac{\partial}{\partial n} + \hat{t}\frac{1}{s_t}\frac{\partial}{\partial t} + \hat{\tau}\frac{1}{s_\tau}\frac{\partial}{\partial \tau} \quad (5)$$

$$= [\hat{x}, \hat{y}, \hat{z}] \; [\mathbf{D}]_3^{n-t-\tau} \begin{bmatrix} \frac{\partial}{\partial x} \\ \frac{\partial}{\partial y} \\ \frac{\partial}{\partial z} \end{bmatrix} \quad (6)$$

DESIGN OF MAPPING SCALES FOR TWO- AND THREE-DIRECTION PMLS

At the edges between two one-direction PMLs, a two-direction PML is needed to 'buffer' mismatch between the two one-direction PMLs, as shown in Fig. 1. To match n_1 PML, along n_1 direction the two-direction PML must use the same scale as that of n_1 PML, s_1. For n_2 PML, s_2 must be used along n_2 direction. When the two directions are not perpendicular to each other, designing the two-direction PML generally becomes more difficult. Fortunately, a simple solution has been found by using a common scale $s = s_1 = s_2$ for both one-direction PMLs. Therefore the common scale can be applied in both directions of the 'buffer' PML. It can be proved that all coplanar two-direction PMLs are equivalent to each other when a common mapping scale is applied in both directions for the PMLs. The equation is directly delivered as follows for brevity. A similar design is used for three-direction PMLs.

$$\nabla_2^{n_1-t_1}(s_{n_1} = s_{t_1} = s) = \nabla_2^{n_2-t_2}(s_{n_2} = s_{t_2} = s) \quad (7)$$

NUMERICAL EXAMPLE

A simple problem having analytical solution is calculated to verify the formulations for the arbitrarily oriented PMLs. A cylindrical wave is applied as incident wave. To save computational costs, only a section between x and y axes is meshed by finite elements. Three one-direction and two 'buffer' PMLs are used to construct an absorbing wall, as shown in Fig. 3. Electromagnetic fields are excited by the boundary condition on the inner boundary. In free space between the inner boundary and the PMLs, a very good agreement between the finite element results and the analytical solution is achieved within an error range of 0.1%.

CONCLUSION

Electromagnetic equations for arbitrarily oriented PMLs are introduced using the complex space mapping method. Configuration of a matched PML structure is discussed. In the calculated example, the good agreement between the numerical and analytical solutions shows that the radiation wave is absorbed by the PML absorber.

ACKNOWLEDGEMENTS

The authors would like to thank Dr C R I Emson and Prof Trowbridge of Vector Fields Ltd for useful help, interesting discussion and allowing the authors to link their subroutines for PML to Vector Fields software, and the EPSRC contract GR/K78744.

References

[1] Jean-Pierre Berenger, "A Perfectly Matched Layer for the Absorption of Electromagnetic Wave", *Journal of Computational Physics*, vol. 114, pp. 185–200, 1994.

[2] Carry M Rappaport, "Perfectly Matched Absorbing Boundary Conditions Based on Anisotropic Lossy Mapping of Space", *IEEE Microwave and Guided Wave Letters*, vol. 5, No. 3, pp. 90–92, March 1995.

[3] Carey M Rappaport, "Interpreting and Improving the PML Absorbing Boundary Condition Using Anisotropic Lossy Mapping of Space", *IEEE Transactions on Magnetics*, vol. 32, No. 3, pp. 968–974, May 1996.

$$
[\mathbf{D}]_1^n = \begin{bmatrix} \frac{n_x^2}{s_n} + t_x^2 + \tau_x^2 & \frac{n_x n_y}{s_n} + t_x t_y + \tau_x \tau_y & \frac{n_x n_z}{s_n} + t_x t_z + \tau_x \tau_z \\ \frac{n_y n_x}{s_n} + t_y t_x + \tau_y \tau_x & \frac{n_y^2}{s_n} + t_y^2 + \tau_y^2 & \frac{n_y n_z}{s_n} + t_y t_z + \tau_y \tau_z \\ \frac{n_z n_x}{s_n} + t_z t_x + \tau_z \tau_x & \frac{n_z n_y}{s_n} + t_z t_y + \tau_z \tau_y & \frac{n_z^2}{s_n} + t_z^2 + \tau_z^2 \end{bmatrix} \tag{8}
$$

$$
= \begin{bmatrix} 1 + (\frac{1}{s_n} - 1) n_x^2 & (\frac{1}{s_n} - 1) n_x n_y & (\frac{1}{s_n} - 1) n_x n_z \\ (\frac{1}{s_n} - 1) n_y n_x & 1 + (\frac{1}{s_n} - 1) n_y^2 & (\frac{1}{s_n} - 1) n_y n_z \\ (\frac{1}{s_n} - 1) n_z n_x & (\frac{1}{s_n} - 1) n_z n_y & 1 + (\frac{1}{s_n} - 1) n_z^2 \end{bmatrix} \tag{9}
$$

$$
[\mathbf{D}]_2^{n-t} = \begin{bmatrix} \frac{n_x^2}{s_n} + \frac{t_x^2}{s_t} + \tau_x^2 & \frac{n_x n_y}{s_n} + \frac{t_x t_y}{s_t} + \tau_x \tau_y & \frac{n_x n_z}{s_n} + \frac{t_x t_z}{s_t} + \tau_x \tau_z \\ \frac{n_y n_x}{s_n} + \frac{t_y t_x}{s_t} + \tau_y \tau_x & \frac{n_y^2}{s_n} + \frac{t_y^2}{s_t} + \tau_y^2 & \frac{n_y n_z}{s_n} + \frac{t_y t_z}{s_t} + \tau_y \tau_z \\ \frac{n_z n_x}{s_n} + \frac{t_z t_x}{s_t} + \tau_z \tau_x & \frac{n_z n_y}{s_n} + \frac{t_z t_y}{s_t} + \tau_z \tau_y & \frac{n_z^2}{s_n} + \frac{t_z^2}{s_t} + \tau_z^2 \end{bmatrix} \tag{10}
$$

$$
[\mathbf{D}]_3^{n-t-\tau} = \begin{bmatrix} \frac{n_x^2}{s_n} + \frac{t_x^2}{s_t} + \frac{\tau_x^2}{s_\tau} & \frac{n_x n_y}{s_n} + \frac{t_x t_y}{s_t} + \frac{\tau_x \tau_y}{s_\tau} & \frac{n_x n_z}{s_n} + \frac{t_x t_z}{s_t} + \frac{\tau_x \tau_z}{s_\tau} \\ \frac{n_y n_x}{s_n} + \frac{t_y t_x}{s_t} + \frac{\tau_y \tau_x}{s_\tau} & \frac{n_y^2}{s_n} + \frac{t_y^2}{s_t} + \frac{\tau_y^2}{s_\tau} & \frac{n_y n_z}{s_n} + \frac{t_y t_z}{s_t} + \frac{\tau_y \tau_z}{s_\tau} \\ \frac{n_z n_x}{s_n} + \frac{t_z t_x}{s_t} + \frac{\tau_z \tau_x}{s_\tau} & \frac{n_z n_y}{s_n} + \frac{t_z t_y}{s_t} + \frac{\tau_z \tau_y}{s_\tau} & \frac{n_z^2}{s_n} + \frac{t_z^2}{s_t} + \frac{\tau_z^2}{s_\tau} \end{bmatrix} \tag{11}
$$

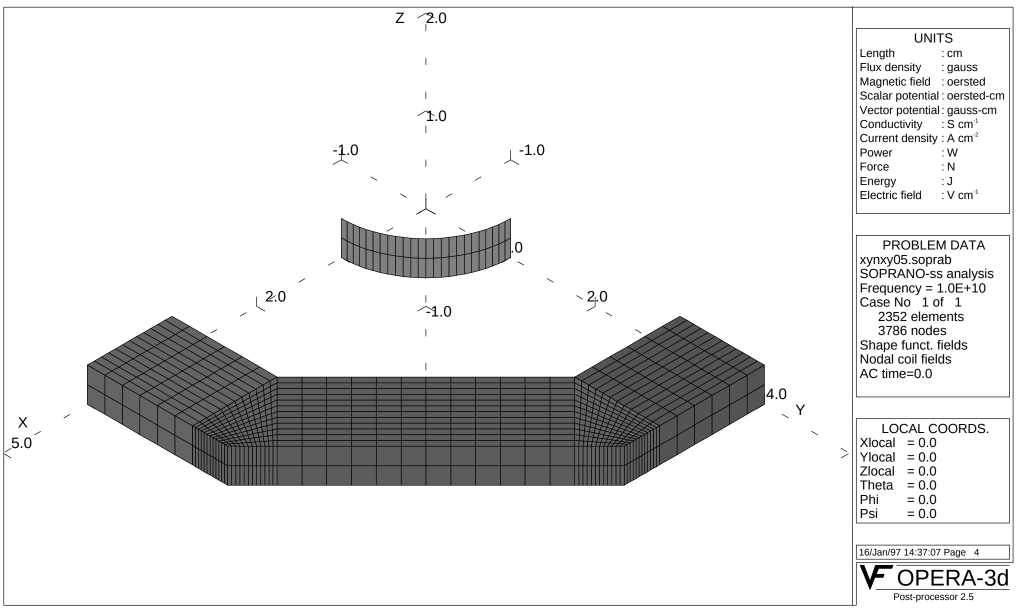

Figure 3: Mesh of Arbitrarily Oriented PML and Inner Boundary Surface